Evaluating the performances of recent detailed combustion mechanisms against NH_3 and NH_3/H_2 experimental data

• • •

András György Szanthoffer[a,b,*], Máté Papp[a], Tamás Turányi[a]

[a] *Institute of Chemistry, ELTE Eötvös Loránd University, Budapest, Hungary*
[b] *Hevesy György PhD School of Chemistry, ELTE Eötvös Loránd University, Budapest, Hungary*

Abstract

There has been a growing interest in utilizing ammonia (NH_3) as a fuel in recent years. Due to ammonia's poor combustion properties, it is often used in combination with hydrogen (H_2) to enhance combustion performance. Over the past decade, several detailed kinetic mechanisms have been developed to model NH_3 and NH_3/H_2 combustion under different conditions. However, no single mechanism has been universally accepted as the most accurate. This study systematically assesses the performance of 24 NH_3 combustion mechanisms published between 2019 and 2024 by examining how accurately they reproduce indirect experimental data. The experimental data collection used for this evaluation includes shock tube ignition delay times (IDT), laminar burning velocities (LBV), and species concentrations measured in shock tubes, jet-stirred reactors, and flow reactors. With a total of 17,242 data points across 1,327 data series from 110 publications, this is, to the best of our knowledge, the most extensive data collection ever employed for NH_3/H_2 mechanism testing. The performance of the mechanisms was assessed based on how many of the experimental data points were reproduced within the 1σ, 2σ, 3σ, etc. uncertainty limits, where σ is the standard deviation of the experimental data. Significant differences were observed between the performance of the different models investigated, and their performance also highly depends on the type of the experiment. The NUIG-2024 mechanism (containing 39 species and 312 reactions) had the best performance for IDT and concentration measurements, where it reproduced 85 and 81% of the experimental data points, respectively, within their 3σ uncertainty limits. However, it ranked only 13th in the case of LBV measurements, and it reproduced only 53% of the LBV data within their 3σ uncertainty limits. For LBV data, the Mathieu-2024 and KAUST-2023 mechanisms reproduced the experimental data the most accurately. Despite its less accurate predictions for LBV data, the NUIG-2024 mechanism can be a good initial mechanism for further mechanism reduction and optimization due to its detailed chemistry and good predictivity for IDT and concentration data.

Keywords: Carbon-free fuel; Ammonia combustion; Detailed chemical kinetic mechanism; Quantitative mechanism comparison; Experimental data collection

---

*Corresponding author.
andras.gyorgy.szanthoffer@ttk.elte.hu

1. Introduction

As climate change accelerates, minimizing carbon dioxide (CO_2) emissions from human activities has become a crucial challenge. One approach to achieving this goal involves utilizing renewable energy sources and carbon-free fuels. Ammonia (NH_3) stands out as a promising carbon-free fuel due to its ability to be synthesized using renewable energy. It offers several advantages, including a high hydrogen density, ease of liquefaction, and an existing infrastructure for storage and transportation. Additionally, its energy density is comparable to that of fossil fuels like methane (CH_4). However, the direct use of NH_3 as a fuel is hindered by its poor combustion properties, such as high ignition energy, low burning velocity, low heat of combustion, and the potential for significant NO_x emissions [1-3].

To overcome these challenges, ammonia is frequently blended with co-fuels such as hydrogen, synthesis gas, methane, gasoline, diesel, kerosene, dimethyl ether (DME), diethyl ether (DEE), methanol, ethanol, dimethoxymethane (DMM), or coal to improve its combustion characteristics [4]. Among these options, hydrogen (H_2) is the most extensively studied due to its carbon-free nature. Beyond its use as a fuel, ammonia also plays a role in the thermal $DeNO_x$ process in the power sector [5].

For the advancement of NH_3-fueled reciprocating engines and gas turbines, accurate chemical kinetic mechanisms are necessary to effectively model the combustion behavior of NH_3 fuel mixtures under conditions of practical applications. Numerous mechanisms have been introduced in the literature to model the oxidation of NH_3/H_2 mixtures [6, 7]. Research by Szanthoffer et al. [6] has shown that while some models align with experimental data under certain conditions, they can significantly diverge in others. Additionally, Rocha et al. [8] highlighted substantial discrepancies among the predictions of different models, emphasizing the need for thorough validation and further refinement of these mechanisms.

Since our previous performance comparison of NH_3 combustion mechanisms [6], numerous new models and additional indirect experimental data have been published in the literature. These were also not included in the study by Girhe et al. [7]. Consequently, the objectives of this study are to i) collect all reliable indirect experimental data on NH_3 and NH_3/H_2 combustion from existing literature; ii) collect all available NH_3 combustion mechanisms; iii) assess the performance of the mechanisms in a quantitative way based on how accurately they can reproduce the experimental results; iv) identify the overall best mechanism.

2. Experimental data collection

Experimental data were utilized in which the fuel was NH_3 or NH_3/H_2, and the oxidizer was O_2, i.e., NO_x species were not allowed in the initial gas mixture. The diluents were N_2, Ar, and/or He, and H_2O was allowed as an additive. In this work, only ST IDT, LBV, and concentration measurements in JSRs, laminar FRs, and STs were utilized in the mechanism comparison. In the case of JSR and FR experiments, the utilized data were always outlet concentration measurements. ST experiments include concentration–time (ct) profile and "characteristic concentration" measurements. Characteristic concentration measurements refer to experiments in which a distinguished point of the measured concentration–time curve was selected (e.g., maximum NO concentration), and in a series of measurements, these selected concentrations were plotted as a function of the independent experimental variable (typically temperature).

LBV measurements may suffer from stretch effects, which should be eliminated experimentally or during the post processing of the measured data by extrapolation. In this study, only those LBV data were utilized when the stretch effects were handled correctly.

Table 1 summarizes the main characteristics of the experimental data collection utilized in the present study. The numbers of data series and data points are shown for each type of experiment. The covered ranges of initial conditions (temperature (T), pressure (p), equivalence ratio (φ), and mole-based percentage of H_2 in the fuel mixture (H_2 % in fuel)) are also provided. In the case of LBV measurements, the temperature values refer to the cold-side temperatures of the flames. The "Collection closure" refers to the date when the experimental data collection was finished for the corresponding type of experiment. Therefore, the utilized data collection can be considered complete until those dates. Altogether, 17,242 experimental data points (in 1,327 data series) were utilized from 110 publications. This data collection is much larger than those used in our previous work [6] (3,770 data points in 350 data series) and in the work of Girhe et al. [7] (5,201 data points) [31].

All data utilized in the present study were encoded in RKD (ReSpecTh Kinetics Data) [9] v2.5 format XML (Extensible Markup Language) data files. This file format is used to store combustion data in the Reaction Kinetics branch of the ReSpecTh database (https://ReSpecTh.hu) [10]. The experimental data utilized in this work were stored in altogether 852 RKD format data files.

3. Mechanisms investigated

24 detailed reaction mechanisms listed in Table 2 were tested against the utilized experimental data collection. In our previous mechanism comparison work [6], the POLIMI-2020 [11], Han-2020 [12], and KAUST-2021 [13] mechanisms performed the best on a much smaller collection of NH_3 and NH_3/H_2 experimental data.

Table 1. Summary of the NH_3 and NH_3/H_2 combustion experiments utilized in this work.

Exp. type	Series	Points	T / K	p / atm	φ	H_2 % in fuel	Collection closure
JSR	334	4917	500–1452	0.99–1.40	0.01–5.19	0–70	11 July 2024
ST-IDT	89	624	1023–2720	1.01–41.65	0.47–2.07	0–70	17 Aug 2024
LBV	445	5093	293–821	0.30–36.58	0.20–2.00	0–100	12 Aug 2024
FR	247	4850	451–1973	0.96–98.69	0.01–23.98	0–91	8 Aug 2024
ST-ct	203	1667	1474–2720	1.15–3.59	0.50–3.46	0–49	2 Sep 2024
ST	9	91	1581–2720	1.15–3.59	0.50–1.84	0–21	2 Sep 2024
∑:	**1327**	**17242**	–	–	–	–	–

Each of these models has been updated since then, and only the updated models (POLIMI-2023, CEU-2022, and KAUST-2023) were used in this study. Four other mechanisms (Konnov-2021, Bertolino-2021, Alturaifi-2022, and NUIG-2024) were tested in our recent study on NH_3/air LBV measurements [14]. The Konnov-2021 model has an updated version [15], but it had inferior performance than Konnov-2021 for NH_3/air LBV data [14]; therefore, the Konnov-2021 model was used in the present study. The ELTE-2024 mechanism was created in [26] for NH_3/air LBV data by adding one reaction from Alturaifi-2022 to CEU-2022. The remaining 16 mechanisms were not used in our previous studies on NH_3 combustion.

Table 2. Detailed reaction mechanisms investigated in this study along with the numbers of species and reactions. The year in the mechanism names refers to the publication year of the corresponding mechanism preceded by the first or corresponding author of the corresponding publication or the institution where the mechanism was created.

Mechanism	Species	Reactions	Ref.
Alzueta-2024	35	232	[16]
ELTE-2024	32	141	[14]
Glarborg-2024	34	233	[17]
Mathieu-2024	35	280	[18]
NUIG-2024	39	312	[19]
SJTU-2024	34	224	[20]
WUT-2024	35	238	[21]
Yin-2024	36	273	[22]
Han-2023	32	171	[23]
KAUST-2023	32	243	[24]
POLIMI-2023	31	203	[25]
Zhou-2023	33	233	[26]
Zhu-2023	33	214	[27]
Shrestha-2023	34	283	[28]
Alturaifi-2022	34	265	[29]
CEU-2022	32	140	[30]
Shrestha-2022	33	270	[31]
SJTU-2022	34	232	[32]
Sun-2022	36	229	[33]
WUT-2022	32	213	[34]
Bertolino-2021	31	203	[35]
Dai-2021	33	211	[36]
Konnov-2021	36	298	[37]
Li-2019	34	252	[38]

4. Methodology

4.1. Simulation details

Simulations were carried out with the Optima++ simulation framework code [39], developed at the ELTE Chemical Kinetics Laboratory. Optima++ reads the RKD format experimental data files, sets up simulation tasks based on their contents, and invokes a combustion simulation package to carry out the simulations. In our present investigations, OpenSMOKE++ [40] and Cantera [41] were used for the simulations. Optima++ also generates figures and computes various metrics about the quality of the reproduction of the experimental data by the investigated mechanisms.

Most JSR experiments were simulated using the isothermal–isobaric PerfectlyStirredReactor solver of OpenSMOKE++. In other cases, the authors specified that their JSR experiments had to be simulated assuming constant heat exchange between the reactor and the external environment ("non-adiabatic"/"non-isothermal" approach). This option is not available in Cantera, and therefore OpenSMOKE++ was used for the JSR simulations. In some cases, when constant heat exchange was considered, temperature and concentration oscillations occurred during the simulations. In our investigations, the time-averages of the concentration values during an oscillation period were taken as simulation results because experimentally, the time-averages of the oscillating concentration values were measured [6].

In most experiments carried out in STs, volume profiles did not need to be considered in the simulations. The exception was the work of Shu et al. [42] because significant pressure rises were observed before the ignitions, especially in the case of longer ignition delay times (i.e. at lower temperatures). More details on ST simulations can be found in our previous work [6].

All FR experiments were simulated with the isothermal–isobaric assumption. In the case of non-premixed FR measurements, the preset inlet temperatures and the corresponding residence times were used. For the premixed FR experiments, the given temperature profiles and the reactor geometries were used as inputs for the simulations. The latter option is not available in Cantera, so OpenSMOKE++ was used for the FR simulations.

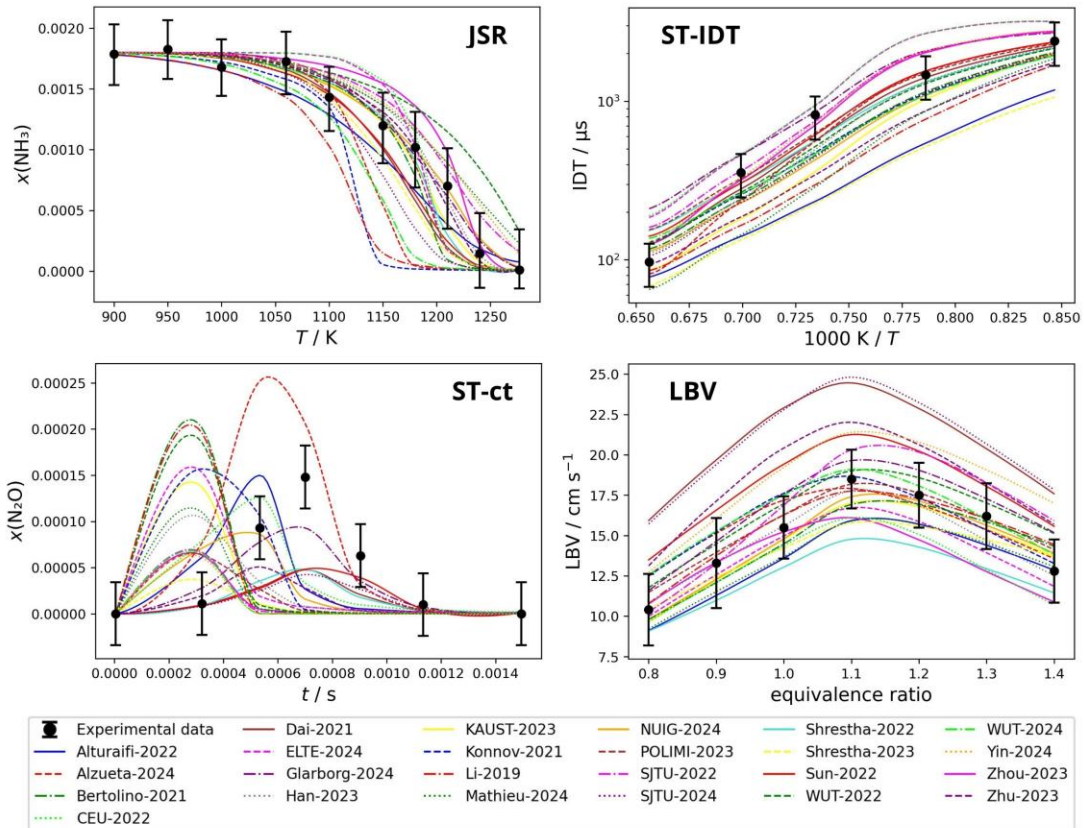

Figure 1. Representative examples of the performance of the mechanisms. Experimentally measured results (symbols) are plotted together with model predictions (lines). Error bars correspond to the 2σ uncertainty limits. Sources of the experimental data are as follows. JSR: Zhang et al. [13]; ST-IDT: Shu et al. [42]; LBV: Lhuillier et al. [43]; ST-ct: Alturaifi et al. [29].

For LBV simulations, the FreeFlame reactor of Cantera was utilized with the following settings. The slope and curvature parameters were set to 0.01 and 0.02, respectively, and the maximum number of grid points was 2000. This resulted in typically 700–1100 grid points in the simulations, which ensured grid-independent solutions. The minimum domain size was set to 3 cm, which resulted in 3–12-cm-long grids in the computations. The Soret effect (thermal diffusion) was included, radiative heat transfer between the flame and the environment was considered via the optically thin model, and the multi-component transport model was applied.

4.2. Quantitative mechanism comparison

The performance of a mechanism is characterized by how accurately it can reproduce the results of indirect experimental measurements. The method applied in this study for quantitative mechanism comparison was suggested by Turányi et al. [44] and has been used successfully for several combustion systems by our research group.

A squared error value can be calculated for each data point in which the square of the difference between the measured and simulated results is normalized by the variance of the corresponding experimental data point:

$$E_{sd} = \left(\frac{Y_{sd}^{\mathrm{exp}} - Y_{sd}^{\mathrm{sim}}}{\sigma\left(Y_{sd}^{\mathrm{exp}}\right)} \right)^2 \tag{1}$$

where

$$Y_{sd} = \begin{cases} y_{sd} & \text{if } \sigma\left(y_{sd}^{\mathrm{exp}}\right) \text{ is absolute error} \\ \ln y_{sd} & \text{if } \sigma\left(y_{sd}^{\mathrm{exp}}\right) \text{ is relative error} \end{cases} \tag{2}$$

Here y_{sd}^{exp} and y_{sd}^{sim} are the measured and simulated values for the *d*-th data point in the *s*-th data series within the data collection, respectively. $\sigma\left(y_{sd}^{\mathrm{exp}}\right)$ is the standard deviation of the corresponding experimental data point. The y_{sd} value is inserted untransformed into Eq. (1) if the corresponding experimental data point is characterized by absolute error. This applies to LBV and concentration measurements [45, 46]. If, however, relative error characterizes the data point, y_{sd} is transformed logarithmically and inserted into Eq. (1). This assumption is applied to IDT measurements

[45, 47]. Consequently, the E_{sd} value is always unitless, and therefore it can be used to compare different types of experimental data. The $\sqrt{E_{sd}}$ value shows how much σ experimental standard deviation the model can reproduce the experimentally measured value.

For a large collection of experimental data, we can investigate the distribution of the $\sqrt{E_{sd}}$ values. In this case, we may say that the mechanism reproducing the most experimental data within their 3σ or 2σ uncertainty limits has the best performance. This approach was used in this work to evaluate the performance of the mechanisms.

5. Results and discussion

In most publications in the literature, the performance of a mechanism is assessed by the visual inspection of figures in which the experimentally measured results are plotted together with model predictions. Some representative plots of this type are shown in Figure 1.

For the quantitative comparison of the performance of the mechanisms, we would like to utilize as many experimental data points as possible. However, it was not possible to use all data points of the data collection for the comparison, because the simulations of some data points did not converge with one or more mechanisms. Not converging simulations occurred almost exclusively in the case of LBV measurements. This can occur due to several reasons, most probably because of numerical problems, e.g. solver issue or the stiffness of the mechanism. To use the same data for each mechanism, the data points whose simulations failed with at least one mechanism were excluded from the mechanism comparison (Criterion 1). Some other data points could not be reproduced within their 3σ uncertainty limits with any of the mechanisms, that is, the $\sqrt{E_{sd}}$ values of these data points were larger than three for all mechanisms. These data points may have very large systematic errors which were not considered, or they are related to experimental conditions that none of the mechanisms can describe satisfactorily. We could not identify which one was the real reason, but these data points were excluded from the quantitative comparison to ensure that the conclusions are unbiased (Criterion 2).

As discussed in section 4.2, the mechanisms are compared based on the ratios of the experimental data points that they can reproduce within given multiples of the standard deviation of the experimental data (1σ, 2σ, 3σ, etc.). This distribution can be visualized in stacked bar plots, as shown in Figure 2. Separate stacked bar plots are shown for the three different measured quantities (concentration, IDT, and LBV) because the numbers of data points in the data collection are very different in the three cases (Table 1). The mechanisms are ordered according to the percentages of the data points that they could reproduce within their 2σ uncertainty limits in descending order (best mechanism on the top). In the case of LBV data, the performance of only 21 mechanisms is shown because, for three mechanisms, more than 5% of the LBV simulations failed (did not converge), which would have resulted in too many excluded data points. These mechanisms are Li-2019 (23.2%), SJTU-2022 (12.2%), and Zhou-2023 (5.5%).

Figure 2 shows that the performance of the mechanisms is relatively similar in the case of concentration measurements, while more significant differences can be observed in the case of IDT and LBV data.

In the case of concentration and IDT data, the best performing model is NUIG-2024. The H_2/O_2 submechanism of NUIG-2024 was taken from NUIGMech1.3 [48] developed at the National University of Ireland, Galway (NUIG) with three updates: reaction $HO_2 + HO_2 = OH + OH + O_2$ was added to NUIGMech1.3 and the rate coefficients of reactions $H_2 + O = H + OH$ and $H + O_2 (+ M) = HO_2 (+ M)$ were updated. The rate coefficients of reactions related to NH_3 oxidation, NO_x formation and consumption, and NH_3/NO_x coupling were selected carefully from the literature. The resulting model was validated against various kinds of experimental data of NH_3 and NH_3/H_2 oxidation and pyrolysis. Figure 2 shows that the NUIG-2024 model has medium performance for LBV data (13th in the list). Note that NUIG-2024 was found to be the best mechanism in the comprehensive mechanism comparison work of Girhe et al. [7].

In the case of LBV data, the Mathieu-2024 and KAUST-2023 mechanisms have the best performance considering the $\leq 2\sigma$ and $\leq 3\sigma$ reproduction ratios, respectively. Mathieu-2024, developed at Texas A&M University, was assembled from different existing submechanisms from the literature. The H_2/O_2 chemistry is from NUIGMech 1.1 [49], the NH_3 pyrolysis submechanism is from Alturaifi et al. [50], and the NH_3/NO_x mechanism was taken from KAUST-2021 [13] with modifications suggested in [29] and [51]. The mechanism was tested only against NH_3 experimental data from the same group at Texas A&M University. Mathieu-2024 has relatively good performance for concentration data (6th) but performs poorly for IDT data (22nd).

The KAUST-2023 model was developed from a previous model, KAUST-2021 [13], of the same research group at King Abdullah University of Science and Technology (KAUST). The KAUST-2021 model is a comprehensive NH_3 and NH_3/H_2 oxidation model validated extensively against experimental data from the KAUST research group and the literature. The important updates of KAUST-2023 on the H_2 and NH_3 oxidation subsets relative to KAUST-2021 are as follows: i) $HO_2 + HO_2$ reactions, ii) isomerization and decomposition reactions of the HONO radical, and iii) bimolecular reactions of HONO isomers with the H atom.

KAUST-2023 performs well for concentration data (3rd) but performs relatively poorly for IDT data (19th).

Based on these considerations, the NUIG-2024 mechanism can be a good initial mechanism for further mechanism optimization and reduction because i) it reproduces concentration and IDT experimental data the best and ii) it contains the most detailed chemistry with 39 species and 312 reactions (Table 2). The mechanism optimization should also include the accurate determination of NH_3 third body collision efficiency parameters and rate coefficients related to the NH_3 pyrolysis subset. The rate parameters of the important H/O reactions may also be tuned, but in that case, a large amount of experimental data on neat H_2 combustion should also be used in the optimization.

6. Conclusions

A comprehensive quantitative comparison of 24 recent detailed NH_3 combustion mechanisms was carried out using a large amount of experimental data on NH_3 and NH_3/H_2 combustion including shock tube ignition delay time (IDT) measurements, concentration measurements in jet stirred and flow reactors and shock tubes, and laminar burning velocity (LBV) measurements. The utilized experimental data collection consists of 17,242 data points in 1,327 data series.

The NUIG-2024 mechanism performed the best for concentration and IDT data, while it had medium performance for LBV data. With 39 species and 312 reactions, this mechanism contains the most detailed chemistry among the investigated models. In the case of LBV data, the Mathieu-2024 and KAUST-2023 mechanisms had the best performance. These mechanisms contain somewhat less detailed chemistry than NUIG-2024, they have good performance for concentration measurements and perform poorly for IDT data. Therefore, NUIG-2024 can be a good initial mechanism for mechanism optimization and reduction. The optimization should include tuning NH_3 third body collision efficiency parameters, rate coefficients related to the NH_3 pyrolysis subset, and, potentially, the rate parameters of the important H/O reactions.

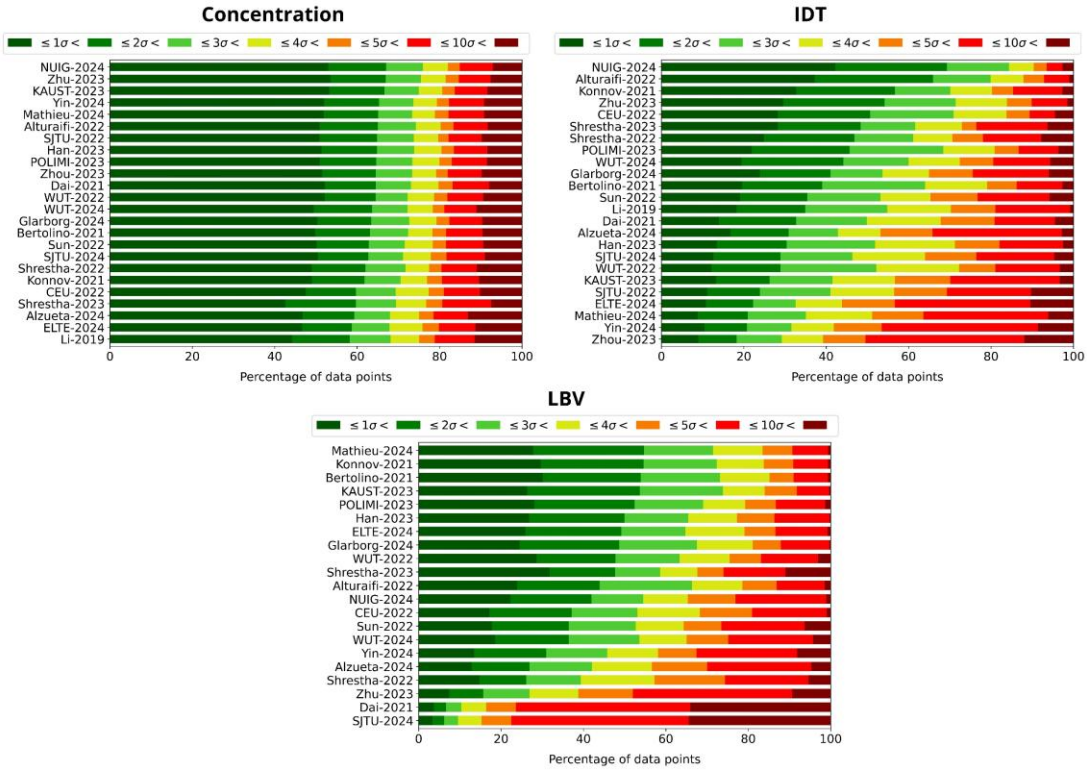

Figure 2. Stacked bar plots showing the percentages of the experimental data points that the mechanisms could reproduce within given thresholds of their standard deviations (σ). Separate stacked bar plots are shown for the different measured quantities (concentration, IDT, and LBV). The mechanisms are ordered according to the $\leq 2\sigma$ reproduction ratio in descending order (best mechanism on the top). The numbers of excluded/included points are as follows. Concentration: 0 (Criterion 1) + 970 (Criterion 2) excluded / 10,555 included; IDT: 1 (Criterion 1) + 26 (Criterion 2) excluded / 597 included; LBV: 145 (Criterion 1) + 10 (Criterion 2) excluded / 4,938 included.

Declaration of competing interest

The authors declare that they have no known competing financial interests or personal relationships that could have appeared to influence the work reported in this paper.

Acknowledgements

This work was supported by NKFIH grant OTKA K147024 of the Hungarian National Research, Development, and Innovation Office. AGySz was supported by the DKOP-23 Doctoral Excellence Program of the Ministry for Culture and Innovation of Hungary from the source of the National Research, Development, and Innovation Fund. We acknowledge the support of COST Action CYPHER CA22151.

Supplementary material

Supplementary material associated with this article is not available.

References

[1] A. Valera-Medina, H. Xiao, M. Owen-Jones, W.I.F. David, P.J. Bowen, Ammonia for power, Prog. Energy Combust. Sci. 69 (2018) 63–102.
[2] H. Kobayashi, A. Hayakawa, K.D.K.A. Somarathne, E.C. Okafor, Science and technology of ammonia combustion, Proc. Combust. Inst. 37 (2019) 109−133.
[3] A. Valera-Medina, F. Amer-Hatem, A.K. Azad, I.C. Dedoussi, M. De Joannon, R.X. Fernandes, P. Glarborg, H. Hashemi, X. He, S. Mashruk, J. Mcgowan, C. Mounaim-Rouselle, A. Ortiz-Prado, A. Ortiz-Valera, I. Rossetti, B. Shu, M. Yehia, H. Xiao, M. Costa, Review on Ammonia as a Potential Fuel: From Synthesis to Economics, Energy Fuels 35 (2021) 6964-7029.
[4] L. Kang, W. Pan, J. Zhang, W. Wang, C. Tang, A review on ammonia blends combustion for industrial applications, Fuel 332 (2023) 126150.
[5] R.K. Lyon, J.E. Hardy, Discovery and development of the thermal $DeNO_x$ process, Ind. Eng. Chem. Fundam. 25 (1986) 19–24.
[6] A.G. Szanthoffer, I.G. Zsély, L. Kawka, M. Papp, T. Turányi, Testing of NH_3/H_2 and NH_3/syngas combustion mechanisms using a large amount of experimental data, Appl. Energ. Combust. Sci. 14 (2023) 100127.
[7] S. Girhe, A. Snackers, T. Lehmann, R. Langer, F. Loffredo, R. Glaznev, J. Beeckmann, H. Pitsch, Ammonia and ammonia/hydrogen combustion: Comprehensive quantitative assessment of kinetic models and examination of critical parameters, Combust. Flame 267 (2024) 113560.
[8] R.C. Da Rocha, M. Costa, X.-S. Bai, Chemical kinetic modelling of ammonia/hydrogen/air ignition, premixed flame propagation and NO emission, Fuel 246 (2019) 24–33.
[9] T. Varga, C. Olm, M. Papp, Á. Busai, A.G. Szanthoffer, I.G. Zsély, T. Nagy, T. Turányi, ReSpecTh Kinetics Data Format Specification v2.5. https://respecth.hu/ReSpecTh_Kinetics_Data_Format_Specification_v2.5.pdf (accessed 29 July 2024).
[10] ELTE Chemical Kinetics Laboratory, MTA-ELTE Complex Chemical Systems Research Group, ReSpecTh Information System. https://ReSpecTh.hu (accessed 29 July 2024).
[11] A. Stagni, C. Cavallotti, S. Arunthanayothin, Y. Song, O. Herbinet, F. Battin-Leclerc, T. Faravelli, An experimental, theoretical and kinetic-modeling study of the gas-phase oxidation of ammonia, React. Chem. Eng. 5 (2020) 696–711.
[12] X. Han, Z. Wang, Y. He, Y. Zhu, K. Cen, Experimental and kinetic modeling study of laminar burning velocities of NH_3/syngas/air premixed flames, Combust. Flame 213 (2020) 1–13.
[13] X. Zhang, S.P. Moosakutty, R.P. Rajan, M. Younes, S.M. Sarathy, Combustion chemistry of ammonia/hydrogen mixtures: Jet-stirred reactor measurements and comprehensive kinetic modeling, Combust. Flame 234 (2021) 111653.
[14] A.G. Szanthoffer, M. Papp, T. Turányi, Identification of well-parameterised reaction steps in detailed combustion mechanisms – A case study of ammonia/air flames, Fuel 380 (2025) 132938.
[15] J. Chen, M. Lubrano Lavadera, A.A. Konnov, An experimental and modeling study on the laminar burning velocities of ammonia + oxygen + argon mixtures, Combust. Flame 255 (2023) 112930.
[16] P. García-Ruiz, I. Salas, E. Casanova, R. Bilbao, M.U. Alzueta, Experimental and Modeling High-Pressure Study of Ammonia–Methane Oxidation in a Flow Reactor, Energy Fuels, doi: 10.1021/acs.energyfuels.3c03959 (2024).
[17] J. Jian, H. Hashemi, H. Wu, P. Glarborg, A.W. Jasper, S.J. Klippenstein, An Experimental, Theoretical, and Kinetic Modeling Study of Post-Flame Oxidation of Ammonia, Combust. Flame 261 (2024) 113325.
[18] O. Mathieu, C.M. Grégoire, E.L. Petersen, Shock-tube study of the oxidation of ammonia by N_2O, Proc. Combust. Inst. 40 (2024) 105250.
[19] Y. Zhu, H.J. Curran, S. Girhe, Y. Murakami, H. Pitsch, K. Senecal, L. Yang, C.-W. Zhou, The combustion chemistry of ammonia and ammonia/hydrogen mixtures: A comprehensive chemical kinetic modeling study, Combust. Flame 260 (2024) 113239.
[20] Z. Zhang, A. Li, Z. Li, F. Ren, L. Zhu, Z. Huang, An experimental and kinetic modelling study on the oxidation of NH_3, NH_3/H_2, NH_3/CH_4 in a variable pressure laminar flow reactor at engine-relevant conditions, Combust. Flame 265 (2024) 113513.
[21] B. Liu, Z. Zhang, S. Yang, F. Yu, B.Y. Belal, G. Li, Experimental and chemical kinetic study for the combustion of ammonia-hydrogen mixtures, Fuel 371 (2024) 131850.
[22] G. Yin, S. Shen, H. Zhan, E. Hu, H. Zhang, Y. Bao, Z. Huang, Experimental and modeling study for the effect of methanol blending on ammonia oxidation and NOx formation at high pressure, Combust. Flame 268 (2024) 113654.
[23] X. Han, Z. Wang, B. Zhou, Y. He, Y. Zhu, K. Cen, Effect of H_2 and O_2 enrichment on the laminar burning velocities of $NH_3+H_2+N_2+O_2$ flames: Experimental and kinetic study, Appl. Energ. Combust. Sci. 15 (2023) 100160.
[24] X. Zhang, K.K. Yalamanchi, S. Mani Sarathy, Combustion chemistry of ammonia/C_1 fuels: A comprehensive kinetic modeling study, Fuel 341 (2023) 127676.
[25] A. Stagni, S. Arunthanayothin, M. Dehue, O. Herbinet, F. Battin-Leclerc, P. Bréquigny, C. Mounaïm-Rousselle, T. Faravelli, Low- and intermediate-temperature ammonia/hydrogen oxidation in a flow reactor: Experiments

and a wide-range kinetic modeling, Chem. Eng. J. 471 (2023) 144577.
[26] S. Zhou, B. Cui, W. Yang, H. Tan, J. Wang, H. Dai, L. Li, Z.u. Rahman, X. Wang, S. Deng, X. Wang, An experimental and kinetic modeling study on NH_3/air, NH_3/H_2/air, NH_3/CO/air, and NH_3/CH_4/air premixed laminar flames at elevated temperature, Combust. Flame 248 (2023) 112536.
[27] S. Zhu, Q. Xu, R. Tang, J. Gao, Z. Wang, J. Pan, D. Zhang, A comparative study of oxidation of pure ammonia and ammonia/dimethyl ether mixtures in a jet-stirred reactor using SVUV-PIMS, Combust. Flame 250 (2023) 112643.
[28] M.V. Manna, P. Sabia, K.P. Shrestha, L. Seidel, R. Ragucci, F. Mauss, M. de Joannon, NH_3–NO interaction at low-temperatures: An experimental and modeling study, Proc. Combust. Inst. 39 (2023) 775–784.
[29] S.A. Alturaifi, O. Mathieu, E.L. Petersen, Shock-tube laser absorption measurements of N_2O time histories during ammonia oxidation, Fuel Comm. 10 (2022) 100050.
[30] S. Wang, Z. Wang, C. Chen, A.M. Elbaz, Z. Sun, W.L. Roberts, Applying heat flux method to laminar burning velocity measurements of NH_3/CH_4/air at elevated pressures and kinetic modeling study, Combust. Flame 236 (2022) 111788.
[31] K.P. Shrestha, B.R. Giri, A.M. Elbaz, G. Issayev, W.L. Roberts, L. Seidel, F. Mauss, A. Farooq, A detailed chemical insights into the kinetics of diethyl ether enhancing ammonia combustion and the importance of NO_x recycling mechanism, Fuel Comm. 10 (2022) 100051.
[32] J. Zhang, B. Mei, W. Li, J. Fang, Y. Zhang, C. Cao, Y. Li, Unraveling Pressure Effects in Laminar Flame Propagation of Ammonia: A Comparative Study with Hydrogen, Methane, and Ammonia/Hydrogen, Energy Fuels 36 (2022) 8528–8537.
[33] Z. Sun, Y. Deng, S. Song, J. Yang, W. Yuan, F. Qi, Experimental and kinetic modeling study of the homogeneous chemistry of NH_3 and NO_x with CH_4 at the diluted conditions, Combust. Flame 243 (2022) 112015.
[34] S. Xu, G. Li, M. Zhou, W. Yu, Z. Zhang, D. Hou, F. Yu, Experimental and kinetic studies of extinction limits of counterflow cool and hot diffusion flames of ammonia/n-dodecane, Combust. Flame 245 (2022) 112316.
[35] A. Bertolino, M. Fürst, A. Stagni, A. Frassoldati, M. Pelucchi, C. Cavallotti, T. Faravelli, A. Parente, An evolutionary, data-driven approach for mechanism optimization: theory and application to ammonia combustion, Combust. Flame 229 (2021) 111366.
[36] L. Dai, H. Hashemi, P. Glarborg, S. Gersen, P. Marshall, A. Mokhov, H. Levinsky, Ignition delay times of NH_3/DME blends at high pressure and low DME fraction: RCM experiments and simulations, Combust. Flame 227 (2021) 120–134.
[37] X. Han, M. Lubrano Lavadera, A.A. Konnov, An experimental and kinetic modeling study on the laminar burning velocity of $NH_3 + N_2O$ + air flames, Combust. Flame 228 (2021) 13–28.
[38] R. Li, A.A. Konnov, G. He, F. Qin, D. Zhang, Chemical mechanism development and reduction for combustion of $NH_3/H_2/CH_4$ mixtures, Fuel 257 (2019) 116059.
[39] M. Papp, T. Varga, Á. Busai, I.G. Zsély, T. Nagy, T. Turányi, Optima++ v2.5: A General C++ Framework for Performing Combustion Simulations and Mechanism Optimization. https://respecth.hu (accessed 29 July 2024).
[40] The CRECK Modeling Group (Politecnico di Milano), OpenSMOKE++: A General Framework Developed for Numerical Simulations of Reacting Systems with Detailed Kinetic Mechanisms, Including Thousands of Chemical Species and Reactions. https://www.opensmokepp.polimi.it/ (accessed 29 July 2024).
[41] D.G. Goodwin, R.L. Speth, H.K. Moffat, B.W. Weber, Cantera: An object-oriented software toolkit for chemical kinetics, thermodynamics, and transport processes, Version 2.5.1, https://www.cantera.org. doi: 10.5281/zenodo.4527812.
[42] B. Shu, S.K. Vallabhuni, X. He, G. Issayev, K. Moshammer, A. Farooq, R.X. Fernandes, A shock tube and modeling study on the autoignition properties of ammonia at intermediate temperatures, Proc. Combust. Inst. 37 (2019) 205–211.
[43] C. Lhuillier, P. Brequigny, F. Contino, C. Mounaïm-Rousselle, Experimental investigation on ammonia combustion behavior in a spark-ignition engine by means of laminar and turbulent expanding flames, Proc. Combust. Inst. 38 (2021) 5859–5868.
[44] T. Turányi, T. Nagy, I.G. Zsély, M. Cserháti, T. Varga, B.T. Szabó, I. Sedyó, P.T. Kiss, A. Zempléni, H.J. Curran, Determination of Rate Parameters Based on Both Direct and Indirect Measurements, Int. J. Chem. Kinet. 44 (2012) 284–302.
[45] C. Olm, I.G. Zsély, T. Varga, H.J. Curran, T. Turányi, Comparison of the performance of several recent syngas combustion mechanisms, Combust. Flame 162 (2015) 1793–1812.
[46] P. Zhang, I.G. Zsély, M. Papp, T. Nagy, T. Turányi, Comparison of methane combustion mechanisms using laminar burning velocity measurements, Combust. Flame 238 (2022) 111867.
[47] P. Zhang, I.G. Zsély, V. Samu, T. Nagy, T. Turányi, Comparison of methane combustion mechanisms using shock tube and rapid compression machine ignition delay time measurements, Energy Fuels 35 (2021) 12329–12351.
[48] S. Panigrahy, A.A.E.-S. Mohamed, P. Wang, G. Bourque, H.J. Curran, When hydrogen is slower than methane to ignite, Proc. Combust. Inst. 39 (2023) 253–263.
[49] M. Baigmohammadi, V. Patel, S. Nagaraja, A. Ramalingam, S. Martinez, S. Panigrahy, A.A.E.-S. Mohamed, K.P. Somers, U. Burke, K.A. Heufer, A. Pekalski, H.J. Curran, Comprehensive Experimental and Simulation Study of the Ignition Delay Time Characteristics of Binary Blended Methane, Ethane, and Ethylene over a Wide Range of Temperature, Pressure, Equivalence Ratio, and Dilution, Energy Fuels 34 (2020) 8808–8823.
[50] S.A. Alturaifi, O. Mathieu, E.L. Petersen, An experimental and modeling study of ammonia pyrolysis, Combust. Flame 235 (2022) 111694.
[51] C.R. Mulvihill, S.A. Alturaifi, E.L. Petersen, A shock-tube study of the $N_2O + M \rightleftarrows N_2 + O + M$ (M = Ar) rate constant using N_2O laser absorption near 4.6 µm, Combust. Flame 224 (2021) 6–13.